Original Article

MOLECULAR METABOLISM

Lateral hypothalamus hypocretin/orexin glucose-inhibited neurons promote food seeking after calorie restriction

Suraj B. Teegala [1,5], Pallabi Sarkar [1], Dashiel M. Siegel [1], Zhenyu Sheng [1,6], Lihong Hao [2], Nicholas T. Bello [2], Luis De Lecea [3], Kevin D. Beck [1,4], Vanessa H. Routh [1,*]

ABSTRACT

Objective: The present study tests the hypothesis that changes in the glucose sensitivity of lateral hypothalamus (LH) hypocretin/orexin glucose-inhibited (GI) neurons following weight loss leads to glutamate plasticity on ventral tegmental area (VTA) dopamine neurons and drives food seeking behavior.

Methods: C57BL/6J mice were calorie restricted to a 15% body weight loss and maintained at that body weight for 1 week. The glucose sensitivity of LH hypocretin/orexin GI and VTA dopamine neurons was measured using whole cell patch clamp recordings in brain slices. Food seeking behavior was assessed using conditioned place preference (CPP).

Results: 1-week maintenance of calorie restricted 15% body weight loss reduced glucose inhibition of hypocretin/orexin GI neurons resulting in increased neuronal activation with reduced glycemia. The effect of decreased glucose on hypocretin/orexin GI neuronal activation was blocked by pertussis toxin (inhibitor of G-protein coupled receptor subunit $G\alpha_{i/o}$) and Rp-cAMP (inhibitor of protein kinase A, PKA). This suggests that glucose sensitivity is mediated by the $G\alpha_{i/o}$-adenylyl cyclase-cAMP-PKA signaling pathway. The excitatory effect of the hunger hormone, ghrelin, on hcrt/ox neurons was also blocked by Rp-cAMP suggesting that hormonal signals of metabolic status may converge on the glucose sensing pathway. Food restriction and weight loss increased glutamate synaptic strength (indexed by increased AMPA/NMDA receptor current ratio) on VTA dopamine neurons and the motivation to seek food (indexed by CPP). Chemogenetic inhibition of hypocretin/orexin neurons during caloric restriction and weight loss prevented these changes in glutamate plasticity and food seeking behavior.

Conclusions: We hypothesize that this change in the glucose sensitivity of hypocretin/orexin GI neurons may drive, in part, food seeking behavior following caloric restriction.

Keywords Electrophysiology; Conditioned-place preference; Dopamine; Glutamate plasticity; Protein kinase A; Ghrelin

1. INTRODUCTION

Caloric restriction and weight loss increase food seeking behavior [1]. The ventral tegmental area (VTA) dopamine neurons promote both drug and food seeking behavior [2]. VTA dopamine neurons receive excitatory input from the lateral hypothalamus (LH) hypocretin/orexin (hcrt/ox) neurons that convey information regarding metabolic status [3]. For example, the activity of hcrt/ox neurons is altered by calorie restriction as well as the metabolic hormones, ghrelin and leptin [4]. Leptin receptor (LepRB)-expressing neurons in the LH exert a powerful monosynaptic inhibitory effect on hcrt/ox cells [5]. LH hcrt/ox neurons are also inhibited by glucose (glucose-inhibited or GI neurons) [6,7]. We showed that the glucose sensitivity of LH hcrt/ox-GI neurons is regulated by metabolic status. The satiety hormone, leptin, enhances and the "hunger" hormone, ghrelin, reduces the inhibitory effect of glucose on the activity of LH hcrt/ox-GI neurons [6]. An overnight fast which increases ghrelin and decreases leptin also reduces glucose inhibition [6]. This reduction in the inhibitory effect of glucose on neuronal activity following calorie restriction would increase the activation of hcrt/ox neurons in response to declines in glycemia. Low glucose and overnight calorie restriction-induced changes in the glucose sensitivity of LH hcrt/ox neurons enhance glutamatergic transmission on VTA dopamine neurons [8]. Moreover, raising LH glucose levels reduces food seeking behavior in calorie restricted rats

[1]Department of Pharmacology, Physiology and Neuroscience, New Jersey Medical School, Rutgers, The State University of New Jersey, Newark, NJ 07103, USA [2]Department of Animal Science, School of Environmental and Biological Sciences, Rutgers, The State University of New Jersey, New Brunswick, NJ 08901, USA [3]Department of Psychiatry and Behavioral Sciences. Wu Tsai Neuroscience Institute. 1201 Welch Rd. Stanford, CA 94305, USA [4]Neurobehavioral Research Laboratory, Research Service, Veterans Affairs New Jersey Health Care System, East Orange, NJ, USA

[5] Present Address: PTC Therapeutics, Piscataway, NJ.
[6] Present Address: Chemistry Faculty, Suffolk County Community College, Seldin, NY.

*Corresponding author. E-mail: routhvh@njms.rutgers.edu (V.H. Routh).

Received May 31, 2023 • Revision received July 5, 2023 • Accepted July 31, 2023 • Available online 2 August 2023

https://doi.org/10.1016/j.molmet.2023.101788

Abbreviations

AAV	Adeno-associated viral vector
aCSF	Artificial cerebrospinal fluid
BIS	Bisindolymaleimide
C21	Compound 21 (DREADD agonist)
CNQX	6-cyano-7-nitroquinoxaline-2,3-dione
CPP	Conditioned place preference
DREADD	Designer receptor exclusively activated by designer drugs
EGFP	Enhanced green fluorescent protein
EPSC	excitatory post-synaptic current
GI	Glucose-inhibited
GPCR	G-protein coupled receptor
Hcrt/ox	hypocretin/orexin
HEPES	N-2-hydroxyethylpiperazine-N′-2-ethanesulfonic acid
Ih	H current
IHC	Immunohistochemistry
IPSC	Inhibitory post-synaptic current
LH	Lateral hypothalamus
MP	Membrane potential
NMDG	N-methyl-D-glucamine
PBS	phosphate buffered saline
PFA	paraformaldehyde
PKA	Protein kinase A
PTX	Pertussis toxin
R	Whole cell resistance
TH	Tyrosine hydroxylase
VTA	Ventral tegmental area

[8]. These data suggest that the glucose sensitivity of LH hcrt/ox-GI neurons may play a role in food seeking behavior following calorie restriction.

The current study tests the hypothesis that, like acute fasting, maintained calorie restriction leading to weight loss similarly reduces glucose inhibition of LH hcrt/ox-GI neurons. Furthermore, weight loss induced changes in the glucose sensitivity of LH hcrt/ox-GI neurons are associated with glutamate plasticity on VTA dopamine neurons and increased food seeking behavior. To test our hypothesis, we determined whether changes in the glucose sensitivity of LH hrct/ox-GI neurons persist following weight loss. We also evaluated the mechanisms by which ghrelin converges on glucose sensing pathways in LH hcrt/ox-GI neurons. We then determined whether chemogenetic inhibition of LH hcrt/ox neurons was sufficient to prevent weight loss induced changes in glutamate plasticity on VTA dopamine neurons and food seeking behavior (evaluated using conditioned place preference; CPP). The results support our hypothesis and suggest that changes in the glucose sensing pathway in LH hcrt/ox-GI neurons may contribute to the increased drive for food seeking behavior following caloric restriction.

2. METHODS

2.1. Animals

Mice with enhanced green fluorescent protein (EGFP) on their Hcrt/ox promotor (Hcrt-EGFP mice) on a C57BL/6J background were provided by Martin G Myers, University of Michigan, Michigan, US. A colony was maintained at Rutgers New Jersey Medical School by crossing male hcrt/ox-EGFP mice to female C57BL/6J mice (Strain # 000664, Jackson laboratories). Supplementary Fig. 1A (S1A) shows a representative coronal brain section from a hcrt/ox-GFP mouse demonstrating expression of EGFP in the dorsomedial, perifornical and lateral hypothalamus. LH hcrt/ox-EGFP neurons were defined by their location lateral to the fornix in the tuberal hypothalamus (Fig. S1A) [9]. EGFP expression was specific to hcrt/ox neurons (Fig. S1B). Hcrt/ox-IRES cre knockin mice on a C57BL/6J background were provided by Luis de Lecea, Stanford University, California, US. A colony was maintained at Rutgers New Jersey Medical School by crossing male hcrt/ox-cre mice to female C57BL/6J mice. Supplementary Figure 4A (S4A) demonstrates cre expression in orexin neurons in these mice. Wild-type C57BL/6J mice were obtained from Jackson laboratories. Male 6 to 8-week-old mice were either group housed or singly housed (calorie restriction experiments) on a 12:12 light—dark cycle (lights out 7.00 PM). Single housed mice were housed 2 per cage with a perforated divider separating them to avoid isolation stress. Mice were fed standard rodent chow (PicoLab Rodent Diet 20 5053) ad libitum unless otherwise specified. Water was provided ad libitum unless otherwise specified. All procedures were in accordance with the Rutgers New Jersey Medical School Institutional Animal Care and Use Committee (IACUC).

2.2. Calorie restriction protocol

Chow intake was monitored for 3 days prior to restriction. The average intake/mouse was ∼4.5—5g. Subsequently, mice were restricted to 85% of their initial body weight by administering 50% of their average chow intake in one daily feeding (2.2—2.5 g, 3—5 PM) of chow immediately after being weighed. This procedure resulted in the mice achieving the target weight loss in ∼7—10 d, after which time the size of their daily meal was titrated (3—3.5 g) to maintain the mice at their reduced body weight for a minimum of 1 week before experimentation. Within experiment, transgenic mice from in-house colonies were age matched and littermates were used when available. C57BL/6J mice were obtained from Jackson laboratories and used in age matched cohorts. Body weights before and after caloric restriction as well as % body weight change for all animals undergoing caloric restriction are listed in Supplementary Table 1.

2.3. Adeno-associated virus (AAV)

Cre dependent AAV-hSyn-DIO-mCherry (50,459-AAV2; Addgene) and AAV-hSyn-DIO-hM4Di-mCherry (44,362-AAV2; Addgene) were purchased from Addgene. AAV-hSyn-DIO-hM4Di-mCherry is a double-floxed Gi-coupled hM4D designer receptor exclusively activated by designer drugs (DREADD) receptor coupled with the mCherry fluorescence marker under the control of a human synapsin promoter. The viral titer obtained from Addgene was $\sim 2.4 \times 10^{12}$ viral genomes (vg)/ml for all viruses and was not diluted.

2.4. Stereotaxic injections

Survival surgeries were performed under anesthesia using a stereotaxic apparatus (Kopf instruments) with digital coordinate system (Nanojet III Programmable Nanoliter Injector, Kopf instruments). Mice were anesthetized with ketamine (80—100 mg/kg)/Xylazine (5—10 mg/kg, intraperitoneally; i.p) followed by buprenorphine (1 mg/kg, subcutaneously; s.c) for analgesia. To minimize pain from scalp incision, bupivacaine (2 mg/kg, s.c) was injected at the site of incision. Hcrt/ox cre mice were injected either with 300 nl of AAV-hSyn-DIO-mCherry or AAV-hSyn-DIO-hM4Di-mCherry per side using the stereotaxic coordinates aimed at the LH (M/L (±) 1.0, A/P (−) 1.24, and (D/V) −5.15. These coordinates target the LH at the level of the fornix in the tuberal hypothalamus [9]. This AAV construct contains a FLEX

switch, which includes loxP and lox2272, to ensure stable expression of hM4Di in cre-expressing cells. All viral injections were made bilaterally. After 2 weeks of recovery from surgery, mice were subjected to the calorie restriction protocol described in section 2.2. Treatment with C21 began on the first day of calorie restriction and continued until the time of sacrifice for both electrophysiological and behavioral studies (approximately 2–3 weeks). DREADD agonist C21 dihydrochloride (Compound 21; water soluble, 10 mg/kg; Cat #HB6124; Hello Bio) was dissolved in distilled water (vehicle) and administered in water bottles. The solution was changed every 3 days. Mice without C21 drank an average of 5 ml/day and mice with C21 drank an average of 4 ml/day. The concentration of C21 was calculated to be 10 mg/kg based on 4 ml/day.

2.5. Electrophysiology

After ~1 week of weight maintenance mice were anesthetized with sodium pentobarbital (60–80 mg/kg, i.p.) and transcardially perfused with ice-cold oxygenated (95%O2/5%CO2) N-methyl-D-glucamine (NMDG) perfusion solution (composition in mM: 110 NMDG, 2.5 KCl, 1.25 NaH_2PO_4, 30 $NaHCO_3$, 20 N-2-hydroxyethylpiperazine-N′-2-ethanesulfonic acid (HEPES), 10 glucose, 2 thiourea, 0.5 $CaCl_2$, 10 $MgSO_4 \cdot 7H_2O$, 5 Na-ascorbate, 3 Na-pyruvate (pH 7.3–7.4, osmolarity adjusted to 310–315 mOsm). Brains were rapidly removed, placed in ice-cold (slushy) oxygenated NMDG perfusion solution and 300 μm coronal slices (containing LH hcrt/ox neurons) or 250 μm horizontal slices (containing LH hcrt/ox and VTA dopamine neurons) were made on a vibratome (7000 smz2, Vibroslice, Camden Instruments, Camden, UK) as previously described [6,8]. The brain slices were then transferred to a pre-warmed (34 °C) initial recovery chamber filled with 150 ml of NMDG perfusion solution. After transferring the slices, Na^+ was reintroduced following the Na^+-spike method [10]. Slices were then transferred to HEPES-artificial cerebrospinal fluid (aCSF) long-term holding chamber (composition in mM: 92 NaCl, 2.5 KCl, 1.25 NaH_2PO_4, 30 $NaHCO_3$, 20 HEPES, 2.5 glucose, 2 thiourea, 5 Na-ascorbate, 3 Na-pyruvate, 2 $CaCl_2 \cdot 2H_2O$, and 2 $MgSO_4 \cdot 7H_2O$ (pH 7.3–7.4, 310–315 mOsm) and allowed to recover for 1 h at room temperature prior to whole-cell current or voltage clamp recording using the recording aCSF (composition in mM: 124 NaCl, 2.5 KCl, 1.25 NaH_2PO_4, 24 $NaHCO_3$, 2.5 glucose, 5 HEPES, 2 $CaCl_2 \cdot 2H_2O$, and 2 $MgSO_4 \cdot 7H_2O$ (pH 7.3–7.4, 310–315 mOsm).

For whole cell current clamp recordings, borosilicate pipettes (4–6 MΩ; Sutter Instruments, Novato, CA) were filled with an intracellular solution containing (in mM): 128 K-gluconate, 10 KCl, 4 KOH, 10 HEPES, 4 $MgCl_2$, 0.5 $CaCl_2$, 5 EGTA, 5 Na_2ATP, and 0.4 Na_2GTP (pH 7.2–7.3, 285–295 mOsm). Cells with membrane potentials more negative than −45 mV in 2.5 mM glucose and action potentials which overshoot 0 mV were considered viable for recording. For cells that did not fire spontaneous action potentials, a depolarizing current was injected at the end of the experiment to check for action potentials. Treatment effects were quantified using whole cell resistance (R, averaging 12 pulses from each treatment during the last minute) and membrane potential (MP, averaging 5 pulses from each treatment) [6,8]. R was calculated from the membrane voltage responses to a −10 or −20 pA hyperpolarizing pulse (500 ms duration). The data were expressed as percent change in response to decreased glucose or ghrelin since there is significant interneuron variability in activity, MP and R depending on the nature of synaptic inputs remaining intact in any given slice preparation and thus, percent change allows specific isolation of the variable being tested (e.g., the response to decreased glucose or to ghrelin addition). Glucose concentrations were varied as described in the figures. In some experiments biocytin (2 mg/ml of intracellular solution) was included in pipette solution for post-recording visualization of the neurons. Spontaneous activity was generated from 'gap-free' acquisition mode using whole cell current clamp method.

For whole cell voltage clamp recordings, pipettes were filled with an intracellular solution containing (in mM): 120 cesium methansulfonate, 20 HEPES, 0.4 EGTA, 2.8 NaCl, 5 TEA-Cl, 2.5 MgATP, and 0.25 NaGTP (pH 7.2–7.3, 285–295 mOsm). Recordings were low pass-filtered at 1 kHz and data were simultaneously digitized at 5 kHz. Pipette access resistance under 30 MΩ with less than a 20% change during the time course of the experiment was considered acceptable. Putative VTA dopamine neurons from wild-type mice were identified by the presence of an H current (Ih). Over 90% of VTA neurons exhibiting a strong Ih are dopamine neurons [11,12]. A strong Ih was defined as a current sag greater than 150 pA at the end of a 500 ms voltage command to −120 mV. To confirm that Ih current positive cells are dopamine cells, recorded neurons were filled with biocytin (2 mg/ml), and slices were saved for post-recording immunohistochemistry (IHC). To stabilize recordings, neurons were first recorded at −60mV holding potential for 5min. Next, to isolate glutamate currents for quantifying AMPAR/NMDAR, neurons were held at a holding potential of +40 mV. Electrically stimulated neurotransmitter release was achieved by placing a concentric bipolar stimulating electrode 100–200 μm rostral to the cell being recorded. Baseline evoked excitatory post synaptic currents (EPSCs) were recorded for 5min in the presence of the GABA-A antagonist bicuculline (20 μm) to block inhibitory post-synaptic currents (IPSCs). Recordings were then made in the presence of the AMPA receptor antagonist CNQX (10 μm; 6-cyano-7-nitroquinoxaline-2,3-dione) along with bicuculline to isolate NMDA currents. Washout was performed after CNQX to check for neuronal viability. The peak current amplitude observed in the presence of CNQX (NMDA) was subtracted from that without CNQX (AMPA + NMDA) to give the AMPA current amplitude. The AMPA/NMDA receptor current ratio was then calculated by dividing the AMPA peak current by the NMDA peak current. Data was generated using the pCLAMP 11 (Molecular Devices, CA) software suite and analyzed with the patch clamp analysis software Clampfit (version 10.7). Using the event detection mode in Clampfit, peak current amplitude for individual currents was obtained. An average of 12 evoked EPSCs from each treatment was used for data analysis.

2.6. Conditioned place preference (CPP)

The CPP apparatus was a two-chamber box with a removable divider separating the chambers. The chambers were discriminated visually by either striped or checked walls and tactually by either a ribbed or smooth floor texture. Mice were habituated to the box with the divider removed for 15 min daily for 5 days. Following habituation, a pretesting phase was performed wherein mice were placed in the open box and the time spent on each side of the chamber was video recorded and measured at 30 min by digital detection software. Using the tracking software designed in house [13], each chamber of the CPP apparatus is divided into two quadrants. A barrier between the two chambers is drawn and the time spent in each quadrant is analyzed using Python code. This is followed by combining the two quadrants on each side to achieve the time spent on each side by the mouse. CPP training began once target weight had been reached. During 8 days of training, mice were restricted on alternating days for 30 min to the chamber of the box in which they initially spent the least amount of time with a food reward or to the chamber where they initially spent the most time without a food reward. We found previously that mice develop a CPP when sweetened cereal (Froot Loops™) was used as a reward [13].

One quarter-piece of cereal in each of the 6 colors of Froot Loops™ was placed along the corners on the less preferred side. This was followed by a final testing phase (post conditioning) during which mice were again placed in the open box for 30 min and the time spent in each chamber was measured. During testing, mice which increased their time (spend at least 55% of time) in the cereal associated chamber (initially less preferred side) were considered to have developed CPP.

2.7. Immunohistochemistry

Mice were anesthetized with sodium pentobarbital (60—80 mg/kg, i.p.) and transcardially perfused with ice-cold 0.01M phosphate buffered saline (PBS) followed by 4% paraformaldehyde (PFA) in PBS. Brains were dissected and post-fixed in 4% PFA/PBS at 4 °C for 24 h, before sequentially undergoing cryoprotection in graded (15% for 24 h followed by 30% (w/v) for 24 h) sucrose solutions in PBS until the tissue specimens completely sank in each solution. The brains were then embedded in optimum cutting temperature and frozen at −80 °C. A series of 30-μm coronal brain slices containing the LHA orexin neurons were obtained using a cryostat (Leica CM 3050S; Leica Microsystems). For post-recording IHC, coronal sections (300 μm) containing the LH hcrt/ox neurons or horizontal sections (250 μm) containing the VTA dopamine neurons were post-fixed in 4% PFA/PBS at 4 °C for 24 h. Following fixation, brain sections were rinsed with 0.01 M PBS (3 times for 10 min), blocked for 90min with 10% bovine serum album (BSA) in 0.3% Triton in 0.01 M PBS, and incubated overnight at 4 °C on an orbital shaker in 5% BSA and 0.3% Triton in 0.01 M PBS containing the primary antibodies. The following day, sections were rinsed in 0.05% PBS tween (3 times for 10 min) and incubated in 5% BSA and 0.3% Triton in 0.01 M PBS containing the secondary antibodies. 30 μm sections were incubated on an orbital shaker at room temperature for 4hrs. 250 and 300 μm sections were incubated at 4 °C on an orbital shaker for 24hrs.

The primary antibody solution was diluted as follows: mouse orexin-A (KK09; Santa Cruz Biotechnology) at 1:800, chicken GFP (A10262; Invitrogen) at 1:500, rabbit TH (65,702; Millipore Sigma) at 1:2000, rabbit Cre (Poly9080; BioLegend) at 1:500 and chicken mCherry (NBP2-25158; Novus Biologicals) at 1:500. The secondary antibody solution was diluted as follows: donkey anti-mouse conjugated with Alexa 594 (A21203; Invitrogen) at 1:2000, donkey anti-mouse conjugated with Alexa 488 (A32766; Invitrogen) at 1:1000, goat anti-chicken conjugated with Alexa-488 (A11039; Invitrogen) at 1:2000, donkey anti-rabbit conjugated with Alexa 488 (A21206; Invitrogen) at 1:2000 or 1:5000, goat anti-chicken conjugated with Alexa-594 (A32759; Invitrogen) at 1:2000. Biocytin was labeled with streptavidin-conjugated to Alexa-594 (S11227; Invitrogen) diluted at 1:2000. Immunostaining was also performed without primary antibodies to control for non-specific binding. Slices were then washed with 0.05% PBS tween (4 times for 10 min) and mounted using prolong gold antifade reagent with or without DAPI. Nuclear staining in 250 and 300 μm slices was performed using Hoechst nuclear stain.

2.8. Blood glucose and plasma ghrelin and leptin measurements

Glucose and hormone levels were measured in ad lib fed and calorie restricted mice between 1030 and 1330 h. No additional food restriction was applied to either group before blood collection. Blood glucose was collected via distal tail laceration and measured by handheld glucometer (Contour Next EZ). Terminal blood was collected by cardiac puncture for measurement of plasma ghrelin and leptin. Ghrelin and leptin were measured via ELISA according to manufacturer instructions (Active Ghrelin: Rat/mouse, Catalog # EZRGRA-90K; Leptin: mouse, Catalog # EZML-82K; Sigma—Aldrich).

2.9. Statistical analysis

Comparisons between groups were made using a paired or independent Student's t-test, two-way ANOVA, or repeated measures two-way ANOVA followed by Tukey's or Sidak's multiple comparisons test as applicable. Values were expressed as mean ± SEM. $p < 0.05$ was considered statistically significant.

2.10. Data availability

Data will be made available by corresponding author upon request

3. RESULTS

3.1. Mechanism of glucose sensing by hcrt/ox-GI neurons

Hcrt/ox-EGFP mice were used to visualize hcrt/ox neurons for whole cell current-clamp recordings. We first confirmed that EGFP expression was specific to hcrt/ox neurons (Figure S1A and S1B). LH hcrt/ox neurons were predominantly quiescent in 2.5 mM glucose, with initiation of action potentials in the majority of neurons as glucose decreased, as shown previously [6]. Since action potential frequency was extremely variable, likely due to other inputs in the brain slice preparation, results were quantified as percentage changes in MP and R in response to decreased glucose or ghrelin. Decreased glucose from 2.5 to 0.1 mM depolarized the MP of LH hcrt/ox-GI neurons by 4.25 ± 0.30% and increased R by 34.45 ± 1.99% (n = 10; Figure 1A). R was calculated from the voltage (V) response to a constant hyperpolarizing current (I) pulse (−10 to −20 pA) using Ohm's law where V=IR (inset in Figure 1A shows representative traces of the voltage response to a constant hyperpolarizing pulse in 2.5 mM and 0.1 mM G on an expanded time scale). An increase in R indicates ion channel closure, whereas a decrease indicates the converse. We and others have previously demonstrated that glucose opens K^+ channels and directly inhibits hcrt/ox-GI neurons, whereas low glucose closes these K^+ channels, as indicated by increased R, and excites hcrt/ox neurons. Glucose sensing is metabolism independent suggesting that these neurons sense the glucose molecule per se [6,13,14]. Thus, we determined whether glucose sensing was mediated by a G-protein coupled receptor (GPCR).

Preincubation of brain slices with 500 ng/ml pertussis toxin (PTX, a GCPR $G\alpha_{i/o}/G\alpha_q$ subunit inhibitor) for 2 h prior to placing them in the patch clamp recording bath significantly reduced the percentage change in MP in response to a maximal glucose decrease from 2.5 mM to 0.1 mM compared to control (control: 8.18 ± 0.51%, number of neurons/number of mice (n/N) = 6/4; PTX: 4.69 ± 0.48%, n/N = 11/11, Independent Student's t-test, $P < 0.001$, $t = 4.58$, $df = 15$, Figure1B). PTX also led to a significant reduction in the percentage change in R compared to control (control: 28.22 ± 2.61%; PTX: 11.51 ± 1.08%; Independent Student's t-test; $p < 0.0001$, $t = 6.97$, $df = 15$, Figure 1B). In contrast, 2 h incubation with PTX had no effect on baseline MP (control: −53 ± 3 mV; PTX -52 ± 2 mV, Independent Student's t-test $P = 0.685$, $t = 0.4142$, $df = 14$) or R (control: 964 ± 106 MΩ; PTX: 1191 ± 71 MΩ, Independent Student's t-test $P = 0.0865$, $t = 1.843$, $df = 14$) in 2.5 mM glucose. Application of the protein kinase C inhibitor, bisindolylmaleimide (BIS; 200 nM) to the patch clamp recording bath had no effect on the response to a glucose decrease from 2.5 to 0.5 mM (Fig. S2). In contrast, application of the PKA inhibitor Rp-cAMP (10 μM) to the patch clamp recording bath blocked the change in MP (control 4.96 ± 0.47%, Rp-cAMP

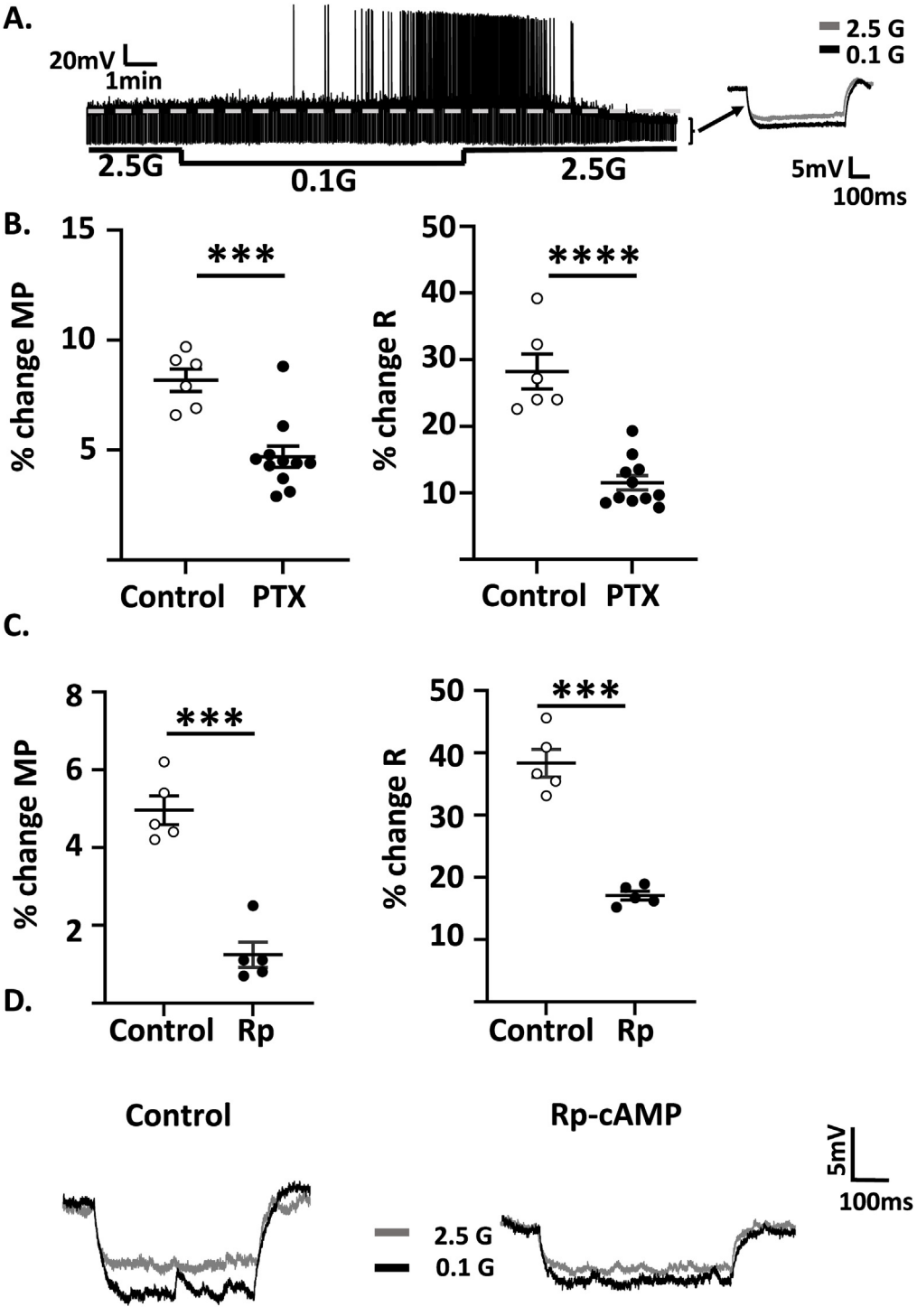

Figure 1: Glucose sensing in hcrt/ox-GI neurons is mediated by protein kinase A (PKA). A. Representative whole cell voltage clamp recording of a hcrt/ox-GI neuron. When extracellular glucose decreased from 2.5 to 0.1 mM, this neuron reversibly depolarized its membrane potential (MP) and increased whole cell resistance (R) and action potential frequency. R was calculated by measuring the voltage response (downward deflection, expanded in inset to the right) to a constant hyperpolarizing current pulse (Ohm's Law: voltage (V) = current (I) x R). B–C. Percent change in MP and R in response to decreased glucose from 2.5 to 0.1 in the presence and absence (control) of: (B) the G-protein coupled receptor blocker, pertussis toxin (PTX, 500 ng/ml); brain slices were incubated in PTX for 2 h prior to recording (control, n/N (# neurons/#mice) = 6/4; PTX, n/N = 11/11, Independent Student's t-test) and (C) the PKA inhibitor, Rp-cAMP (10 μM; Rp) added to the bath solution (n/N = 5/5, Paired Student's t-test).***$P < 0.001$, ****$P < 0.0001$. D. Representative voltage responses to decreased glucose in the presence and absence of Rp-cAMP (gray: 2.5, black 0.1 mM glucose). Data represented as mean ± SEM.

1.24 ± 0.32, Paired Student's t-test; $P < 0.001$, $t = 13.46$, $df = 4$, n/N = 5/5) and R (control 38.34 ± 2.21%, Rp-cAMP 17.06 ± 0.69, Paired Student's t-test, $P < 0.001$, $t = 11.03$, $df = 4$) in these neurons in response to decreased glucose from 2.5 to 0.1 mM glucose (Figure 1C,D). Addition of Rp-cAMP to 2.5 mM glucose had no effect on baseline MP (control: −74 ± 1 mV; Rp-cAMP −75 ± 1 mV, Paired Student's t-test $P = 0.422$, $t = 0.8930$, $df = 4$) or R (control: 420 ± 46 MΩ; Rp = cAMP: 414 ± 49 MΩ, Paired Student's t-test $P = 0.219$, $t = 1.457$, $df = 4$).

3.2. Effect of calorie restriction and weight loss maintenance

We showed previously that an overnight fast decreased the inhibitory effect of glucose on LH hcrt/ox-GI neurons [6]. Here, we determined whether this change in glucose sensitivity persisted during caloric restriction to 85% of original body weight and maintenance of that weight for 1 week. A subset of mice had terminal blood collected to measure blood glucose and plasma ghrelin and leptin levels. Glucose levels were significantly reduced in calorie restricted mice both at their target weight and after weight loss maintenance (Figure 2A). As expected, plasma ghrelin levels were significantly higher in calorie restricted mice compared to ad lib fed controls (ad lib: 115.2 ± 28.0 pg/ml, $n = 7$; calorie restricted (CR): 338.2 ± 41.1 pg/ml, $n = 10$; Independent Student's t-test $P = 0.001$, $t = 4.074$, $df = 15$, Figure 2A). Similarly, plasma leptin levels were reduced in calorie restricted vs ad lib fed mice (ad lib: 2.29 ± 0.36 ng/ml, $n = 8$, CR: 0.39 ± 0.04 ng/ml, Independent Student's t-test $P < 0.0001$, $t = 5.59$, $df = 15$, Figure 2A). At the time of sacrifice, these calorie restricted mice weighed −12.36 ± 0.09% less than their starting weight ($n = 10$). In this experiment, glucose levels were reduced from 2.5 to 0.7 mM during patch clamp recording to mimic the change in hypothalamic glucose levels after an overnight fast [15]. Calorie restriction significantly increased the MP change in response to decreased glucose from 2.5 to 0.7 mM. glucose compared to the ad-lib fed group (ad lib: 3.55 ± 0.19%, n/N = 5/5, CR: 4.14 ± 0.10%, n/N = 5/4, $p < 0.05$, Independent Student's t-test, $t = 2.67$, $df = 8$, Figure 2B). The percentage change in R in response to decreased glucose also increased with calorie restriction compared to the control treatment (ad lib: 30.55 ± 2.31%; CR: 41.26 ± 0.55%, $p < 0.01$, Independent Student's t-test, $t = 4.5$, $df = 8$, Figure 2B). Thus, like fasting [16], calorie restriction decreased the inhibitory effect of glucose on hcrt/ox-GI neurons. We next determined whether ghrelin signaling also converged on the PKA pathway. The addition of ghrelin (10 nM) to 2.5 mM glucose (glucose concentration held constant) increased MP and R of hcrt/ox neurons (Figure 2C). Bath application of Rp-cAMP (10 μM) significantly reduced this percentage change in MP in response to 10 nM ghrelin compared to control (control: 3.07 ± 0.06%, n/N = 6/5; Rp-cAMP (Rp): 0.71 ± 0.14%, n/N = 5/5 $p < 0.0001$, Independent Student's t-test, $t = 16.15$, $df = 9$, Figure 2C). The ghrelin-induced change in R was also reduced by the PKA inhibitor compared to the control treatment (control: 20.70 ± 0.73%; Rp-cAMP: 7.39 ± 0.84%, $p < 0.0001$, Independent Student's t-test, $t = 11.94$, $df = 9$, Figure 2C).

We showed previously that low glucose activates VTA dopamine neurons in a hcrt/ox dependent manner and causes a persistent increase in AMPAR and NMDAR currents on VTA dopamine neurons in vitro [8]. Thus, we determined whether calorie restriction also increased glutamate currents on VTA dopamine neurons. To retain the connection between LH and VTA, we made voltage clamp recordings in horizontal brain sections as described previously [6]. VTA dopamine neurons were initially identified by the presence of a strong hyperpolarization-activated inwardly rectifying non-specific cation current (H-current, Ih; Fig. S3A) as described previously [6,8]. To confirm that Ih current positive cells are dopaminergic, we filled recorded neurons with biocytin for post-recording immunohistochemistry to determine if they expressed tyrosine hydroxylase (TH; Fig. S3B). Any neurons that were TH negative were dropped from the data analysis. Interestingly, of the 66 Ih positive neurons, only 8 were not TH positive. This is consistent with previous studies of VTA DA neurons [11,12]. This suggests that the Ih is a reasonable marker for VTA dopamine neurons. There was a significant increase in the AMPA receptor current amplitude (pA) in calorie restricted mice compared to the ad-lib fed controls (ad lib: 17.62 ± 2.74, n/N = 8/5, CR: 38.03 ± 3.17, n/N = 8/4; $p < 0.001$, Independent Student's t-test, $t = 4.87$, $df = 14$, Figure 3A). In contrast, there was no significant difference in the NMDA receptor current amplitude between the ad-lib fed (n/N = 8/5) and calorie restricted (n/N = 8/4) groups (Figure 3A). This led to a significant increase in the AMPA/NMDA receptor current ratio in the calorie restricted mice compared to the ad-lib fed controls (ad lib: 0.64 ± 0.08, CR: 1.18 ± 0.1 $p < 0.01$, Independent Student's t-test, $t = 4.09$, $df = 14$, Figure 3B). Next, we used CPP to determine whether calorie restriction had a similar effect on food seeking behavior. While both calorie restricted and ad lib fed mice developed CPP for a food reward, food seeking behavior (as indexed by increased time in the food associated chamber of the CPP box) was significantly greater in calorie restricted mice (Repeated measures 2-way ANOVA; Interaction between diet state and time in the food associated chamber: $P = 0.045$, $F(1,14) = 4.815$ Figure 3C).

3.3. Hcrt/ox mediates the effect of calorie-restriction on VTA dopamine glutamate currents and the motivation to seek rewarding food

We selectively inhibited hcrt/ox neurons using DREADDs. 6-week-old mice expressing cre-recombinase on the hcrt/ox promoter (hcrt/ox cre mice) were stereotactically injected into the LH with either cre-dependent control (AAV-hSyn-DIO-mCherry) or inhibitory (AAV-hSyn-DIO-hM4Di-mCherry) virus. We confirmed expression of cre recombinase in the hcrt/ox neurons in the hcrt/ox-cre mice (Fig. S4A) and expression of mCherry virus in hcrt/ox neurons (Fig. S4B and C). We further confirmed that activation of hM4Di with the DREADD agonist, C21 (1 μM), inhibited hcrt/ox neurons (Fig. S5). All mice were subjected to the calorie restriction protocol and provided with C21 (10 mg/kg) or vehicle in their drinking water for the duration of calorie restriction. There were no significant differences in absolute current amplitude (pA) in either AMPA or NMDA receptor current between the groups (Two-way ANOVA, Tukey's post-hoc test, $p > 0.05$, Figure 4A). However, there was a significant interaction (Two-way ANOVA, $P = 0.035$, ($F(1, 29) = 6.023$) between the AAVs and C21 for the AMPA/NMDA receptor current ratio (Figure 4 B, C). Tukey's multiple comparisons post hoc test revealed a significant decrease in AMPA/NMDA receptor current ratio in mice injected with hM4Di and treated with C21 (0.73 ± 0.02, n/N = 8/4) compared to the other 3 groups, which did not differ from one another (control virus treated with vehicle: 0.95 ± 0.03, n/N = 8/4 or C21: 0.97 ± 0.06, n/N = 9/5 and the hM4Di group treated with vehicle: 0.95 ± 0.05, n/N = 8/5; Fig. B, C). In these experiments C21 (1 μM) was included in the recording solution for both mCherry- and hM4Di-C21 groups to mimic the chronic exposure of the treated mice to C21 in subsequent behavioral studies. A caveat to this paradigm is that the presence of C21 during the recording could cause an acute reduction of the AMPA/NMDA receptor current ratio. To address this issue, we determined whether the decreased AMPA/NMDA receptor current ratio persisted when C21 was not included in the recording solution. We found no significant

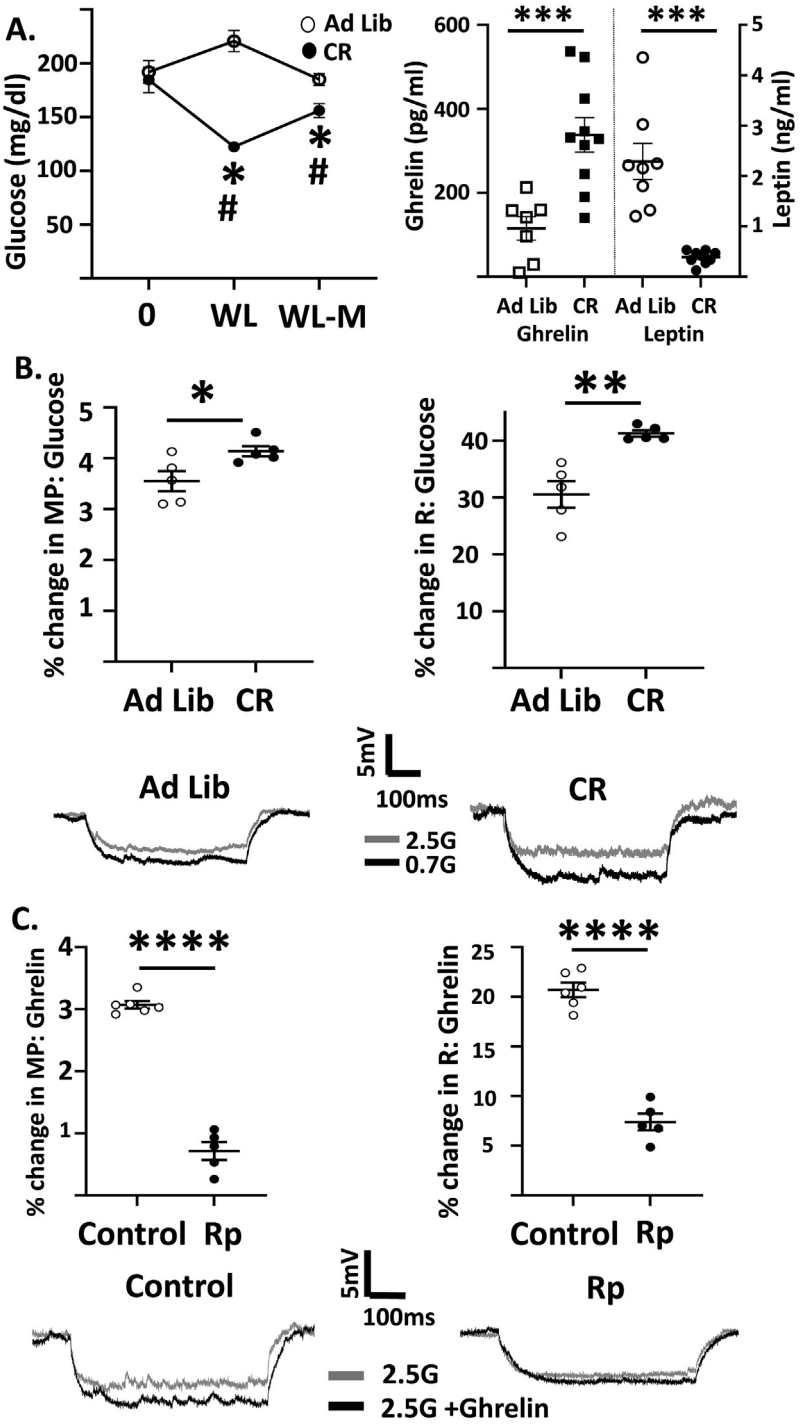

Figure 2: Calorie restriction decreases glucose inhibition of hcrt/ox-GI neurons due, in part, to ghrelin action on PKA. A. Blood glucose levels (left) were measured in a subset of ad lib fed and calorie restricted (CR) mice at the start of the study (time 0), upon reaching ~15% weight loss (WL) and after 1-week WL-maintenance (WL-M). Plasma glucose levels were lower during WL and WL-M (Repeated measures 2-way ANOVA showed an interaction between diet status and time ($P < 0.0001$, $F(2,36) = 17.26$); Sisak's multiple comparison *$P < 0.05$ CR compared to time 0 within their group, #$P < 0.01$ CR compared to the same time point for the ad lib fed group ($n = 10$/group). Plasma ghrelin levels (right) were significantly higher in these CR mice at the end of WL-M (Independent Student's t-test ***$P < 0.001$, $t = 4.074$, $df = 15$, $n = 7$ ad lib, $n = 10$ CR) and plasma leptin levels (far right) were significantly lower (Independent Student's t-test ***$P < 0.0001$, $t = 5.59$, $df = 15$, $n = 8$ ad lib, $n = 9$. CR). B. Top: Percent change in MP and R of hcrt/ox-GI neurons in response to decreased glucose from 2.5 to 0.7 in ad lib fed and CR mice (Independent Student's t-test, *$P < 0.05$, **$P < 0.01$, ad lib n/N = 6/5, CR n/N = 5/5). Bottom: Representative voltage responses of hcrt/ox-GI neurons to decreased glucose in ad lib and CR mice (gray: 2.5, black 0.1 mM glucose). C. Top: Percent change in MP and R of hcrt/ox neurons in response to the addition of ghrelin (10 nM) to a constant glucose level of 2.5 mM in the presence and absence of the PKA inhibitor Rp-cAMP (10 μM Rp, independent Student's t-test, ****$P < 0.0001$, control n/N = 5/5, Rp-cAMP n/N = 6/5). Bottom: Representative voltage responses to ghrelin addition to 2.5 mM glucose in control and Rp-cAMP (gray: 2.5, black 0.1 mM glucose). Data represented as mean ± SEM.

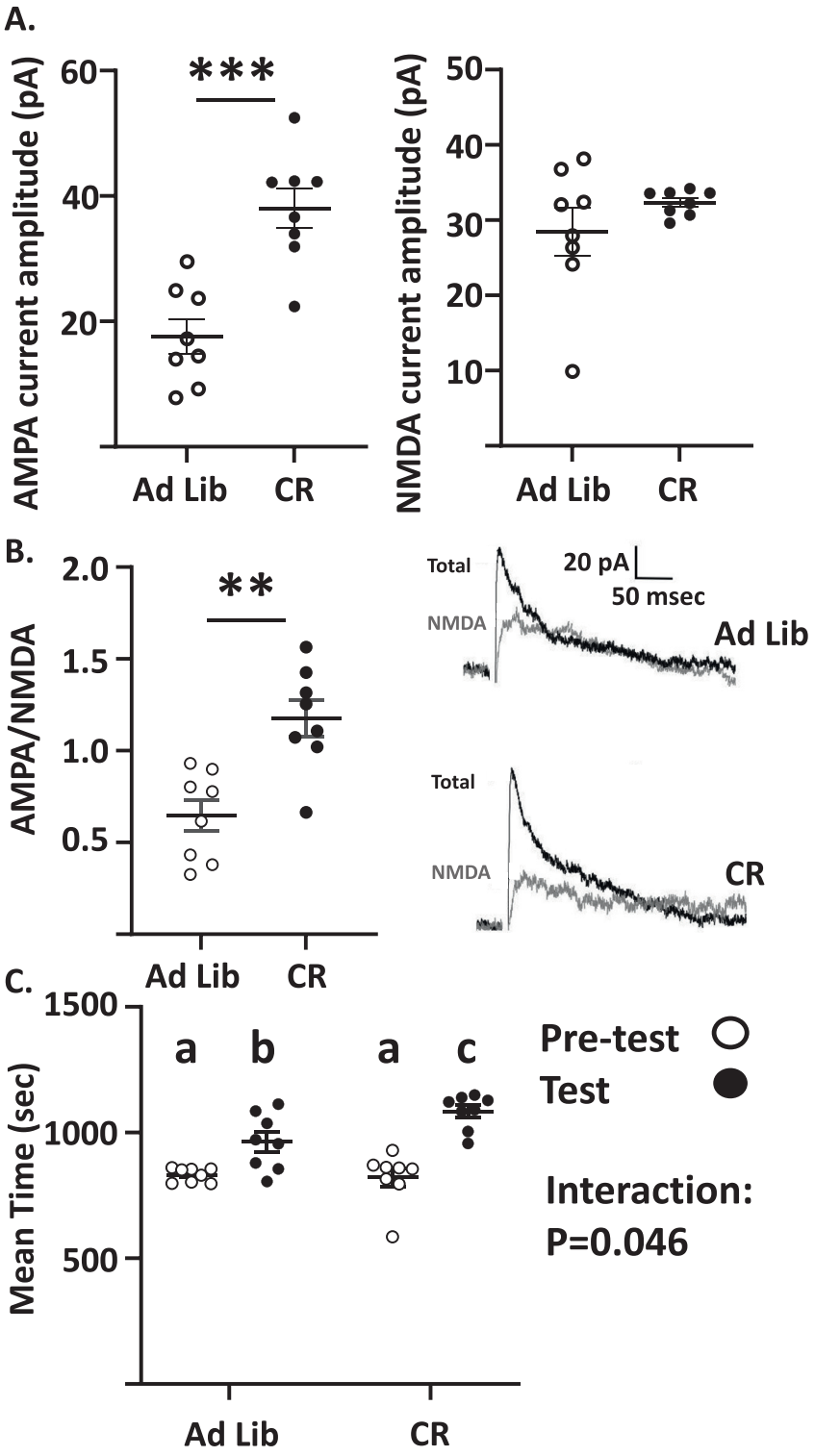

Figure 3: Calorie restriction increases glutamatergic signaling onto VTA dopamine neurons and conditioned place preference (CPP) for a food reward. A. Calorie Restriction significantly increased α-amino-3-hydroxy-5-methyl-4-isoxazolepropionic acid (AMPA; left) but not N-methyl-D-aspartate (NMDA, right) receptor current amplitude. B. Left: Calorie Restriction significantly increased the AMPA/NMDA receptor current ratio. Independent Student's t-test, ad lib n/N = 8/5, calorie restricted (CR) n/N = 8/4, $^{**}P < 0.01$, $^{***}P < 0.001$. Right: Representative voltage clamp recordings of total (black) and NMDA receptor (grey) currents at a holding potential of 40 mV. NMDA currents were recorded in the presence of the AMPA inhibitor cyanquixaline (CNQX, 10 μM). AMPA currents were obtained by subtracting NMDA from total currents. C. Mean time spent on the food reward associated side of a CPP box for ad lib fed and CR mice before (pre-test) and after (test) conditioning for the food reward. Both ad lib fed and CR mice spent more time on the food reward associated side; however, CR mice spent significantly more time than did ad lib fed mice. Repeated measures 2-way ANOVA, Sidak's multiple comparison test; interaction between diet state and conditioning ($F(1, 14) = 4.815$, $p < 0.05$). Different letters indicate that groups are statistically different from each other ($P < 0.05$). Data represented as mean ± SEM.

difference in the AMPA (without C21: 31.02 ± 2.33 pA, n/N = 9/4, with C21 29.26 ± 1.69 pA, n/N = 8/4, Independent Student's t-test, $P > 0.05$, $t = 0.5966$, $df = 15$) or NMDA (without C21: 41.33 ± 2.80 pA, with C21: 40.07 ± 2.81 pA, Independent Student's t-test, $P > 0.05$, $t = 0.3817$, $df = 15$) receptor current amplitude between the groups which had C21 in the bath compared to the group that were not bath perfused with C21. Furthermore, there was no significant difference in the AMPA/NMDA between the groups which had C21 in the bath compared to the group that were not bath perfused with C21 (without C21: 0.75 ± 0.035, with C21: 0.73 ± 0.023, Independent Student's t-test, $P > 0.05$, $t = 0.4401$, $df = 15$; Figure 4D). These data suggest that calorie restriction induces long-term changes in glutamatergic currents on VTA DA neurons, and this effect is mediated by hcrt/ox neurons.

Next, we examined whether CPP after calorie restriction was mediated by hcrt/ox neurons. 6-week-old hcrt/ox-cre mice were injected with either control or hM4Di virus. 2-weeks later, mice were calorie restricted to 85% body weight and weight loss was maintained until the end of the experiment. Mice were divided into 4 groups and treated with vehicle or C21 (10 mg/kg) in their drinking water at the initiation of calorie restriction. When preference before and after conditioning was compared between groups, mean time spent on food associated side was significantly higher after conditioning in all groups except the hM4Di group treated with C21 (Paired Student's t-test comparing mean time on the food preferred side before and after conditioning for each treatment group $P < 0.05$, Figure 5A). This indicates that all groups except those in which hcrt/ox neurons were inhibited developed CPP. We quantified the mean time spent on the food associated side after conditioning and compared it between the 4 groups. Two-way ANOVA revealed that there was a significant interaction between the AAVs and C21 ($(F (1, 29) = 13.04$, $p < 0.01$). Tukey's multiple comparisons post-hoc test demonstrated that there was a significant decrease in the mean time spent on the food associated side in hM4Di mice treated with C21 (888.0 ± 29.95 s, $N = 9$) compared to control mice treated with vehicle (1061 ± 33.42 s, $N = 8$, $p < 0.05$) or C21 (1084 ± 33.60 s, $N = 8$, $p < 0.01$) and hM4Di mice treated with vehicle (1149 ± 56.47 s, $N = 8$, $p < 0.001$, Figure 5B). Next, we quantified the mean percentage time on the food associated side after conditioning and compared it between the groups. Two-way ANOVA revealed that there was a significant interaction between the AAVs and C21 ($(F (1, 29) = 14.77$, $p < 0.0001$). Tukey's multiple comparisons post-hoc test demonstrated that there was a significant decrease in the mean percentage time spent on the food associated side after conditioning in hM4Di mice treated with C21 (47.00 ± 1.55) compared to control mice treated with vehicle (56.05 ± 1.43, $p < 0.05$) or C21 (57.79 ± 1.71, $p < 0.01$) and hM4Di mice treated with vehicle (60.72 ± 3.01, $p < 0.001$, Figure 5C). Figure 5C also reveals that in mice injected with hM4Di and treated with C21, the mean percentage time spent by the animals in the food associated side of the CPP box was approximately 50% indicating equal preference for both sides of the box. This suggests that hcrt/ox signaling to reward associated brain regions is necessary for CPP to positive reinforcers and that inhibiting these neurons results in a failure to attain CPP to food reward.

4. DISCUSSION

The present study shows that an ~15% body weight loss reduces the glucose sensitivity of hcrt/ox-GI neurons, leading to increased activation as glucose levels decline. This is associated with increased glutamate synaptic strength (as indexed by increased AMPA/NMDA receptor current ratio) on VTA dopamine neurons and an increased motivation to seek food (as indexed by CPP). Chemogenetic inhibition of hcrt/ox neurons during food restriction and weight loss prevents these changes in glutamate plasticity and food seeking behavior. Furthermore, our data suggest that elevated plasma ghrelin levels during weight loss may activate the PKA pathway and enhance the effects of low glucose, leading to increased activation of hcrt/ox-GI neurons. Increased activation of hcrt/ox-GI neurons, in turn, would increase excitatory drive onto VTA dopamine neurons and enhance the motivation to seek food. We hypothesize that this change in the glucose sensitivity of hcrt/ox-GI neurons may drive, in part, food seeking following calorie restriction and weight loss.

Hcrt/ox neurons are metabolically regulated. For example, ghrelin and fasting increase while leptin and glucose decrease the activity hcrt/ox neurons [6,7,17]. We previously showed that the glucose sensitivity of hcrt/ox-GI neurons is also regulated by metabolic state. Ghrelin and fasting reduce, while leptin enhances glucose sensitivity of hcrt/ox-GI neurons [6]. Hcrt/ox neurons are multifunctional and have been linked to several behavioral states including addiction and arousal [18–21]. Interestingly, recent data suggest that while orexin neurons are important for food seeking behavior, this food seeking may disrupt or reduce actual food intake [22,23]. How the glucose sensitivity of hcrt/ox neurons impacts these roles is not clear. However, our data show that increased activation of hcrt/ox-GI neurons during energy or glucose deprivation increases food seeking behavior. Our data also suggest that changes in the glucose sensitivity of hcrt/ox-GI neurons may be associated with the increased arousal associated with calorie restriction [24]. Additionally, given the stimulatory role of hcrt/ox in locomotion, we cannot rule out an effect of hcrt/ox inhibition affecting food seeking behavior secondarily to decreased locomotion [21]. An interesting sequelae of our study is the possibility that caloric restriction and weight loss could enhance other forms of rewarding or addictive behavior including that of drug addiction [25]. This could be especially relevant for current health issues given the incidence of eating disorders especially in young females as well as increased problems with drug addiction in economically challenged individuals experiencing food insecurity [26,27].

For these reasons it is important to determine the mechanism of glucose sensing by hcrt/ox-GI neurons. Burdakov and colleagues have attempted to determine the K^+ channel responsible for glucose sensing. While the identity of the specific ion channel has proven elusive, these investigators have narrowed it down to the family of tandem pore K^+ channels [28,29]. In this study, we focused on the intracellular signaling pathway which mediates glucose sensing. Hcrt/ox neurons sense glucose directly in a metabolism independent manner suggesting a glucose receptor [6,13,14]. We hypothesized that the glucose receptor may be a GCPR. Our data showing that the $G\alpha_{i/o}/G\alpha_q$ subunit inhibitor PTX blunted glucose sensing supports this notion. However, PTX did not completely abolish glucose sensing, suggesting that either a longer preincubation was needed (>2 h) or that multiple signaling pathways are involved. PKA inhibition blocked activation of hcrt/ox neurons in low glucose suggesting that the $G\alpha_{i/o}$-adenylyl cyclase-cAMP-PKA pathway is involved. PKA inhibits tandem pore K^+ channels [30,31]. Thus, glucose, via $G\alpha_{i/o}$, would reduce PKA levels and open these K^+ channels leading to inhibition of hcrt/ox-GI neurons. Conversely, decreased glucose increases PKA, closing K^+ channels and activating these neurons. This is consistent with the increased R observed in low glucose that we have previously shown to reflect decreased K^+ conductance [6]. Further work remains to determine which tandem pore channel is specifically responsible for glucose sensing in hcrt/ox-GI neurons. Similarly, our data suggest that PKC inhibition did not block glucose sensing (Fig. S2); however, sample size was small and further

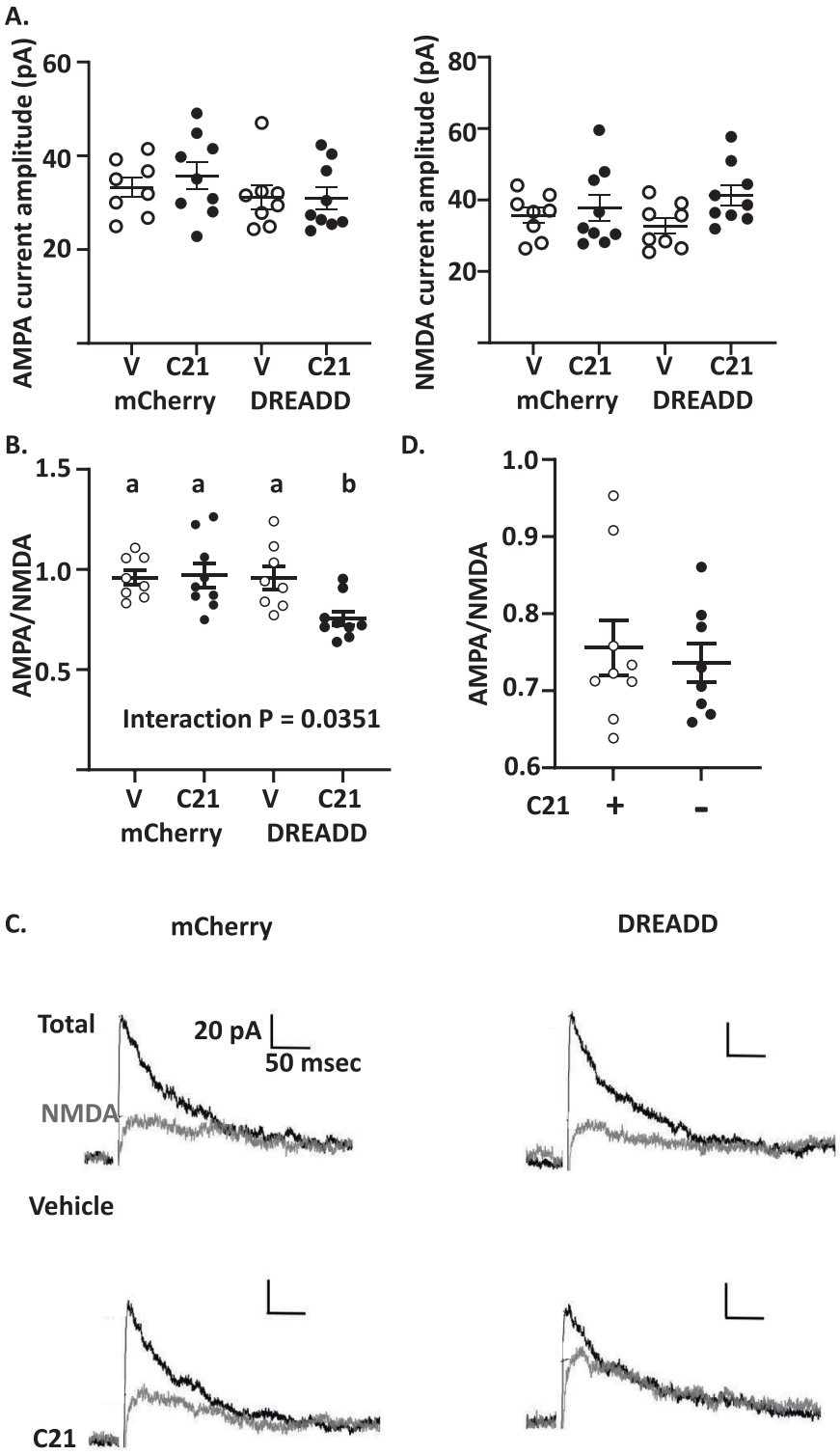

Figure 4: Orexin mediates the effect of caloric restriction on glutamate currents on VTA dopamine neurons. A. There were no significant differences in AMPA or NMDA receptor current amplitude on VTA dopamine neurons from calorie restricted (CR) mice injected with control (pAAV-hSyn-DIO-mCherry) or inhibitory (pAAV-hSyn-DIO-hM4D(Gi)-mCherry) virus and given C21 (10 mg/kg) or vehicle (distilled water) in their drinking water (Two-way ANOVA followed by Tukey's post-hoc test, $P > 0.05$). B. The AMPA/NMDA receptor current ratio was significantly reduced in CR mice injected with the inhibitory DREADD and provided C21. Different letters indicate that groups are statistically different from each other ($P < 0.05$) (Two-way ANOVA followed by Tukey's post-hoc test, interaction between AAV and treatment ($F(1, 29) = 6.023$, $p < 0.05$). Control-vehicle n/N = 8/4, control-C21 n/N = 9/5, Inhibitory DREADD-vehicle n/N = 8/5, Inhibitory DREADD-C21 n/N = 8/4. C. Representative voltage clamp recordings of total (black) and NMDA receptor (grey) currents at a holding potential of 40 mV. NMDA currents were recorded in the presence of the AMPA inhibitor cyanquixaline (CNQX, 10 μM). AMPA currents were obtained by subtracting NMDA from total currents. D. AMPA/NMDA receptor current ratio in VTA dopamine neurons from CR mice injected with the inhibitory DREADD and provided C21 in their drinking water in the presence (C21+, n/N = 8/4) or absence (C21-, n/N = 9/4) of C21 in the recording bath. There were no significant differences between the groups (Independent Student's t-test). Data represent mean ± SEM.

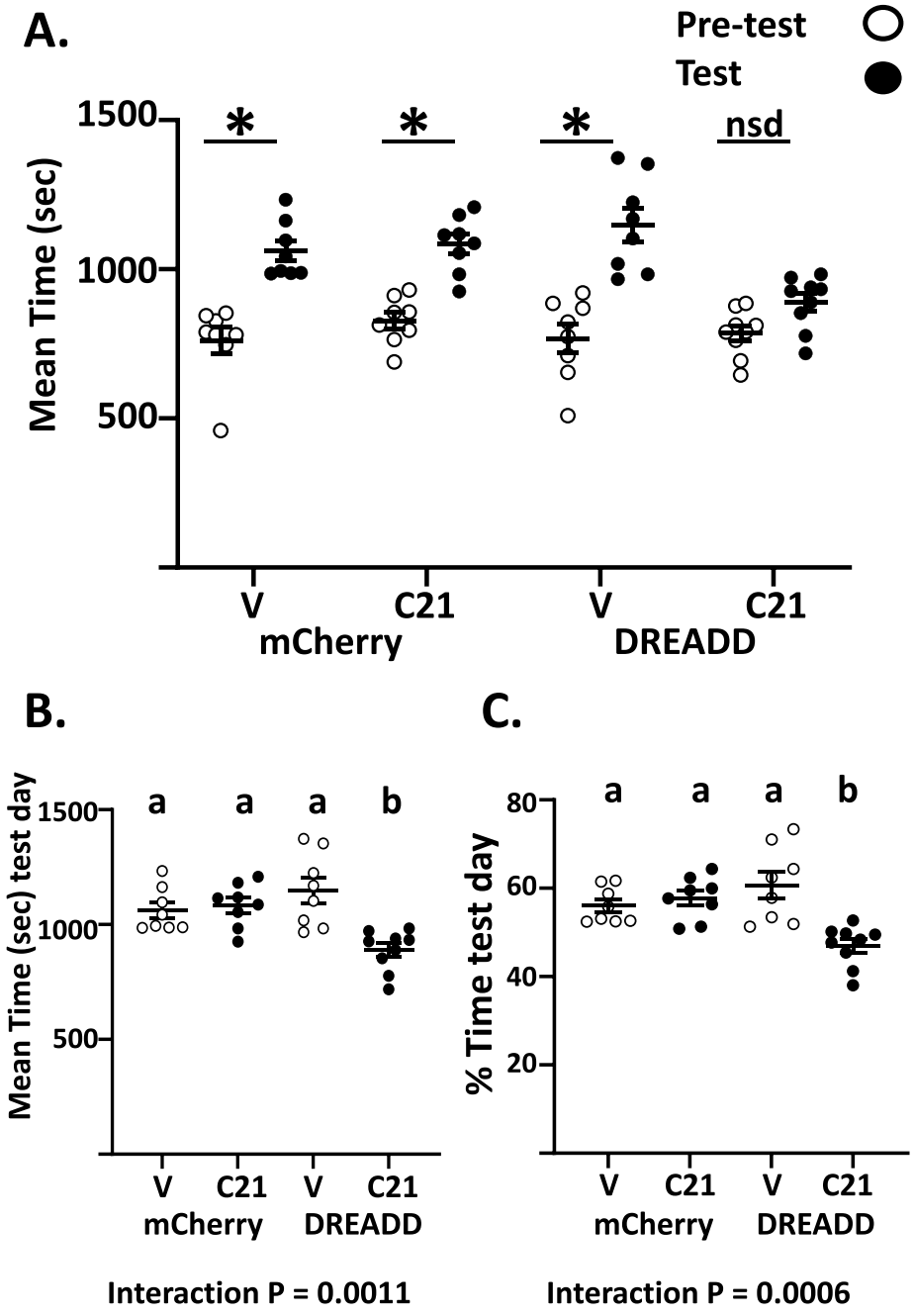

Figure 5: Orexin mediates the effect of calorie restriction on CPP. A. When compared before (pretest) and after (test) conditioning for a food reward, mean time spent on food associated side (sec) was significantly higher in all groups except the hM4Di group treated with C21 (Paired Student's t-test pre-test vs test for each group, *P $<$ 0.05, nsd: not significantly different). B. Mean time spent on the food associated side. Two-way ANOVA showed an interaction between C21 treatment and AAV ((F (1, 29) $=$ 13.04, p $<$ 0.01). Tukey's post-hoc test showed a significant decrease in the mean time spent on the food associated in hM4Di mice treated with C21 (n $=$ 9) compared to control mice treated with vehicle (n $=$ 8) or C21 (n $=$ 8) and hM4Di mice treated with vehicle (n $=$ 8). C. Mean percentage time on the conditioned side on the testing day. Two-way ANOVA showed a significant interaction between C21 treatment and AAV ((F (1, 29) $=$ 14.77, p $<$ 0.01). Tukey's post-hoc test showed a significant decrease in the mean percentage time spent on the food associated side in hM4Di mice treated with C21 compared to control mice treated with vehicle or C21 and hM4Di mice treated with vehicle. The mean percentage time in C21 treated mice injected with hM4Di in the food associated side was close to 50%, suggesting a failure to attain place conditioning to food-reward. Different letters indicate that groups are statistically different from each other (P $<$ 0.05).

study is needed before the conclusion can be drawn that PKC is not involved in glucose sensing. Interestingly, the effect of ghrelin on hcrt/ox neurons in 2.5 mM glucose was also mediated by PKA. We were unable to determine whether the effects of ghrelin on glucose sensing were PKA mediated because the inhibitor blocked glucose sensing almost entirely, making discrimination impossible. However, therapeutic uses for adenylyl cyclase inhibitors are being investigated, raising the possibility of clinical relevance for this potentially convergent gut hormones and glucose sensing pathway [32].

We previously showed that decreased glucose increased glutamate currents on VTA dopamine neurons using a horizontal brain slice containing the LH and VTA. In these studies, the hcrt/ox receptor

antagonist, SB334867, blocked the effect of both low glucose and electrical stimulation of the LH on glutamate currents [6]. This strongly supports our hypothesis that the glucose sensitivity of LH hcrt/ox-GI neurons is relevant for glutamate signaling onto VTA dopamine neurons. In the present study, we found that, like acute fasting, calorie restriction increased the AMPA receptor currents and the AMPA/NMDA receptor current ratio on VTA dopamine neurons. The AMPA/NMDA receptor current ratio is an index of glutamate synaptic strength [33,34]. The effect of calorie restriction on the AMPA/NMDA receptor current ratio was blocked by chemogenetic inhibition of hcrt/ox neurons. Surprisingly, neither AMPA nor NMDA receptor currents individually showed significant effects of chemogenetic inhibition of hcrt/ox neurons. One potential explanation for this is that the individual currents reflect the mean values of all neurons evaluated, whereas the AMPA/NMDA receptor current ratio compared these currents within individual neurons. Thus, an effect that might have obscured in a group average was manifest when the relationship between currents was evaluated within a single neuron. A limitation of our preparation is that we cannot definitively conclude that this was due to inhibition of hcrt/ox-GI neurons (as opposed to the subpopulation of hcrt/ox neurons that are not glucose sensing [6]). However, taken with our earlier data the present studies strongly suggest that glucose sensing by hcrt/ox neurons plays a prominent role in regulating reward circuitry.

These changes in glutamate synaptic strength paralleled the motivation to seek food. That is, calorie restriction increased the time that calorie restricted mice spent in the food associated side of the CPP box relative to ad lib fed animals and this was blocked by chemogenetic inhibition of hcrt/ox neurons. Interestingly, mice in which hcrt/ox neurons were inhibited failed to develop CPP as shown by a lack of conditioning in Figure 5A. This was further evidenced by the observation that they spent half of the time in the food associated chamber (Figure 5C) and so by deduction, half of their time in the non-food associated chamber. A limitation of the CPP as a test of food motivation is that it does not measure the willingness to work for a food reward as could be done using behavioral economics [35]. However, it is clear from our results that calorie restriction enhances food seeking in a hcrt/ox dependent manner. Another limitation for both our behavioral and electrophysiological experiments is that for calorie restriction and chemogenetic inhibition of hcrt/ox neurons, it is necessary for the mice to be single housed to control intake of food and/or C21 (likewise controls were also single housed). Single housing is clearly an isolation stressor and we have found it to raise blood glucose levels (unpublished observations and [13]). At the present time there is no way around this limitation; however, we attempted to mitigate isolation stress by housing the animals in divided cages separated by perforated plastic where they have visual, auditory, and olfactory input from their cage mate. While isolation stress may contribute to the relatively high blood glucose levels in Figure 2A, calorie restriction clearly lowered blood glucose compared to the ad lib fed controls and thus, differences in blood glucose would impact hcrt/ox-GI neurons in this study. A final limitation of this study was that only male mice were used. We have previously shown sexual differentiation in GI neurons of the ventromedial hypothalamus [36,37], thus future studies should be conducted in both sexes.

5. CONCLUSIONS

Hormonal changes associated with calorie restriction and weight loss (e.g., increased ghrelin levels) may converge on the PKA signaling pathway in hcrt/ox-GI neurons. This is associated with a reduction in the inhibitory effect of glucose on these neurons leading to increased activation in response to smaller decreases in blood glucose. This increase in hcrt/ox transmission onto VTA dopamine neurons increases glutamate synaptic strength. Increased glutamate synaptic strength on VTA dopamine neurons, in turn, increases the motivation to seek food. These changes in the glucose sensitivity of hcrt/ox-GI neurons may thus contribute to increased food seeking behavior following caloric restriction and weight loss.

STUDY APPROVAL

All animal procedures were reviewed and approved by the Rutgers University Institutional Animal Care and Use Committee (protocol 0999900906). The mice were maintained in accordance with university guidelines for the care and use of laboratory animals.

AUTHOR CONTRIBUTIONS

SBT and VHR conceived the study. SBT, ZS, LH, PS and DMS conducted the experiments and acquired the data. SBT and VHR analyzed the data. LDL provided hcrt/ox-cre mice. LDL, NTB and KDB provided invaluable scientific input. VHR wrote the manuscript. All authors reviewed, edited if desired, and approved the final version of the manuscript.

DECLARATION OF COMPETING INTEREST

The authors declare that they have no known competing financial interests or personal relationships that could have appeared to influence the work reported in this paper.

DATA AVAILABILITY

Data will be made available on request.

ACKNOWLEDGEMENTS

National Institutes of Health 1RO1 DK103676 (VHR, KDB), Department of Defense W81XWH-19-1-0016 (VHR, NTB)

APPENDIX A. SUPPLEMENTARY DATA

Supplementary data to this article can be found online at https://doi.org/10.1016/j.molmet.2023.101788.

REFERENCES

[1] Fulton S. Appetite and reward. Front Neuroendocrinol 2010;31:85–103.
[2] Fields HL, Hjelmstad GO, Margolis EB, Nicola SM. Ventral tegmental area neurons in learned appetitive behavior and positive reinforcement. Annu Rev Neurosci 2007;30:289–316.
[3] Choi DL, Davis JF, Fitzgerald ME, Benoit SC. The role of orexin-A in food motivation, reward-based feeding behavior and food-induced neuronal activation in rats. Neuroscience 2010;167:11–20.
[4] Sakurai T. Roles of orexins in regulation of feeding and wakefulness. Neuroreport 2002;13:987–95.
[5] Bonnavion P, Mickelsen L, Fujita A, de Lecea L, Jackson AC. Hubs and spokes of the lateral hypothalamus: cell types, circuits and behaviour. J Physiol 2016;54(22):6443–62.

[6] Sheng Z, Santiago AM, Thomas MP, Routh VH. Metabolic regulation of lateral hypothalamic glucose-inhibited orexin neurons may influence midbrain reward neurocircuitry. Mol Cell Neurosci 2014;62:30–41.
[7] Burdakov D, Gerasimenko O, Verkhratsky A. Physiological changes in glucose differentially modulate the excitability of hypothalamic melanin-concentrating hormone and orexin neurons in situ. J Neurosci 2005;25:2429–33.
[8] Teegala SB, Sheng Z, Dalal MS, Hirschberg PR, Beck KD, Routh VH. Lateral hypothalamic orexin glucose-inhibited neurons may regulate reward-based feeding by modulating glutamate transmission in the ventral tegmental area. Brain Res 2020;1731:1445808.
[9] Paxinos G, Franklin KBJ. The mouse brain in stereotaxic coordinates. San Diego: Academic Press; 2003.
[10] Ting JT, Lee BR, Chong P, Soler-Llavina G, Cobbs C, Koch C, et al. Preparation of acute brain slices using an optimized N-methyl-D-glucamine protective recovery method. J Vis Exp 2018;132:53825.
[11] Korotkova TM, Brown RE, Sergeeva OA, Ponomarenko AA, Haas HL. Effects of arousal- and feeding-related neuropeptides on dopaminergic and GABAergic neurons in the ventral tegmental area of the rat. Eur J Neurosci 2006;23:2677–85.
[12] Korotkova TM, Sergeeva OA, Eriksson KS, Haas HL, Brown RE. Excitation of ventral tegmental area dopaminergic and nondopaminergic neurons by orexins/hypocretins. J Neurosci 2003;23:7–11.
[13] Patel V, Sarkar P, Siegel DM, Teegala SB, Hirschberg PR, Wajid H, et al. The anti-narcolepsy drug modafinil reverses hypoglycemia unawareness and normalizes glucose sensing of orexin neurons in male mice. Diabetes 2022. https://doi.org/10.2337/db22-0639 [Online ahead of print].
[14] Gonzalez JA, Jensen LT, Fugger L, Burdakov D. Metabolism-independent sugar sensing in central orexin neurons. Diabetes 2008;57:2569–76.
[15] De Vries MG, Arseneau LM, Lawson ME, Beverly JL. Extracellular glucose in rat ventromedial hypothalamus during acute and recurrent hypoglycemia. Diabetes 2003;52:2767–73.
[16] Sheng Z, Santiago AM, Thomas MP, Routh VH. Metabolic regulation of lateral hypothalamic glucose-inhibited orexin neurons may influence midbrain reward neurocircuitry. Molecular and cellular neurosciences 2014;62:30–41.
[17] Yamanaka A, Beuckmann CT, Willie JT, Hara J, Tsujino N, Mieda M, et al. Hypothalamic orexin neurons regulate arousal according to energy balance in mice. Neuron 2003;38:701–13.
[18] de Lecea L, Carter ME, Adamantidis A. Shining light on wakefulness and arousal. Biol Psychiatr 2012;71:1046–52.
[19] Rao Y, Mineur YS, Gan G, Wang AH, Liu Z-W, Wu X, et al. Repeated in vivo exposure of cocaine induces long-lasting synaptic plasticity in hypocretin/orexin-producing neurons in the lateral hypothalamus in mice. J Physiol 2013;591:1951–66.
[20] Cason AM, Smith RJ, Tahsili-Fahadan P, Moorman DE, Sartor GC, Aston-Jones G. Role of orexin/hypocretin in reward-seeking and addiction: implications for obesity. Physiol Behav 2010;100:419–28.
[21] Harris GC, Aston-Jones G. Arousal and reward: a dichotomy in orexin function. Trends Neurosci 2006;29:571–7.
[22] Viskaitis P, Arnold M, Garau C, Jensen LT, Fugger L, Peleg-Raibstein D, et al. Ingested non-essential amino acids recruit brain orexin cells to suppress eating in mice. Curr Biol 2022;32:1812–1821.e4.
[23] González JA, Jensen LT, Iordanidou P, Strom M, Fugger L, Burdakov D. Inhibitory interplay between orexin neurons and eating. Curr Biol 2016;26:2486–91.
[24] Jiménez A, Caba M, Escobar C. Food-entrained patterns in orexin cells reveal subregion differential activation. Brain Res 2013;1513:41–50.
[25] Carr KD. Modulatory Effects of food restriction on brain and behavioral effects of abused drugs. Curr Pharmaceut Des 2020;26:2363–71.
[26] Herzog DB, Franko DL, Dorer DJ, Keel PK, Jackson S, Manzo MP. Drug abuse in women with eating disorders. Int J Eat Disord 2006;39:364–8.
[27] Basile G. The drug abuse scourge and food insecurity: outlining effective responses for an underestimated problem. Clin Ter 2022;173:299–300.
[28] Burdakov D, Jensen LT, Alexopoulos H, Williams RH, Fearon IM, O'Kelly I, et al. Tandem-pore K+ channels mediate inhibition of orexin neurons by glucose. Neuron 2006;50:711–22.
[29] González JA, Jensen LT, Doyle SE, Miranda-Anaya M, Menaker M, Fugger L, et al. Deletion of TASK1 and TASK3 channels disrupts intrinsic excitability but does not abolish glucose or pH responses of orexin/hypocretin neurons. Eur J Neurosci 2009;30:57–64.
[30] Roy A, Derakhshan F, Wilson RJ. Stress peptide PACAP engages multiple signaling pathways within the carotid body to initiate excitatory responses in respiratory and sympathetic chemosensory afferents. Am J Physiol Regul Integr Comp Physiol 2013;304:R1070–84.
[31] García G, Méndez-Reséndiz KA, Oviedo N, Murbartián J. PKC- and PKA-dependent phosphorylation modulates TREK-1 function in naïve and neuropathic rats. J Neurochem 2021;157:2039–54.
[32] Pierre S, Eschenhagen T, Geisslinger G, Scholich K. Capturing adenylyl cyclases as potential drug targets. Nat Rev Drug Discov 2009;8:321–35.
[33] Bonci A, Borgland S. Role of orexin/hypocretin and CRF in the formation of drug-dependent synaptic plasticity in the mesolimbic system. Neuropharmacology 2009;56(1):107–11.
[34] Harada M, Pascoli V, Hiver A, Flakowski J, Lüscher C. Corticostriatal activity driving compulsive reward seeking. Biol Psychiatr 2021;90:808–18.
[35] Giannotti G, Mottarlini F, Heinsbroek JA, Mandel MR, James MH, Peters J. Oxytocin and orexin systems bidirectionally regulate the ability of opioid cues to bias reward seeking. Transl Psychiatry 2022;12:432.
[36] Santiago AM, Clegg DJ, Routh VH. Estrogens modulate ventrolateral ventromedial hypothalamic glucose-inhibited neurons. Mol Metabol 2016;5:823–33.
[37] Santiago AM, Clegg DJ, Routh VH. Ventromedial hypothalamic glucose sensing and glucose homeostasis vary throughout the estrous cycle. Physiol Behav 2016;167:248–54.

